applied sciences

MDPI

Article

Multiservice Loss Models in Single or Multi-Cluster C-RAN Supporting Quasi-Random Traffic

Iskanter-Alexandros Chousainov [1], Ioannis Moscholios [1,*], Panagiotis Sarigiannidis [2] and Michael Logothetis [3]

1 Department Informatics & Telecommunications, University Peloponnese, 221 00 Tripolis, Greece; ichousain@uop.gr
2 Department Electrical & Computer Engineering, University W. Macedonia, 501 00 Kozani, Greece; psarigiannidis@uowm.gr
3 Department Electrical & Computer Engineering, University Patras, 265 04 Patras, Greece; mlogo@upatras.gr
* Correspondence: idm@uop.gr

Abstract: In this paper, a cloud radio access network (C-RAN) is considered where the baseband units form a pool of computational resource units and are separated from the remote radio heads (RRHs). Based on their radio capacity, the RRHs may form one or many clusters: a single cluster when all RRHs have the same capacity and multi-clusters where RRHs of the same radio capacity are grouped in the same cluster. Each RRH services the so-called multiservice traffic, i.e., calls from many service classes with various radio and computational resource requirements. Calls arrive in the RRHs according to a quasi-random process. This means that new calls are generated by a finite number of mobile users. Arriving calls require simultaneously computational and radio resource units in order to be accepted in the system, i.e., in the serving RRH. If their requirements are met, then these calls are served in the (serving) RRH for a service time which is generally distributed. Otherwise, call blocking occurs. We start with the single-cluster C-RAN and model it as a multiservice loss system, prove that the model has a product form solution, and determine time congestion probabilities via a convolution algorithm whose accuracy is validated with the aid of simulation. Furthermore, the previous model is generalized to include the more complex case of more than one clusters.

Keywords: cloud-radio access; cluster; time congestion; quasi-random; product form; convolution

Citation: Chousainov, I.-A.; Moscholios, I.; Sarigiannidis, P.; Logothetis, M. Multiservice Loss Models in Single or Multi-Cluster C-RAN Supporting Quasi-Random Traffic. *Appl. Sci.* **2021**, *11*, 8559. https://doi.org/10.3390/app11188559

Academic Editor: Fabrizio Granelli

Received: 7 August 2021
Accepted: 29 August 2021
Published: 15 September 2021

1. Introduction

The cloud radio access network (C-RAN) architecture is considered to be a promising and, at the same time, cost-effective solution to face the increasing wireless traffic as well as the soaring demand for enhanced data rate and decreased latency [1,2].

In the C-RAN, a base station is separated into two different parts: (a) the radio frequency components and the antenna which form the so-called remote radio head (RRH) that is in charge of the signal's transmission/reception (e.g., modulation, analog-to-digital and digital-to-analog conversion, as well as power amplification) and (b) the baseband unit (BBU) which is in charge of the baseband signal processing and the communication with the core network.

To guarantee, via the C-RAN architecture, quality of service (QoS) to the mobile users (MUs), it is necessary to deploy, in remote sites, many RRHs of certain radio resource units (RRUs) and at the same time form a pool of BBUs, often located in a cloud data center. Such a pooling reduces the baseband processors as well as the power consumption and the overall operators' capital/operational expenditures [3,4]. Among other advantages of BBU pooling, we mention the possibility of many operators sharing the same BBU pool as well as the more convenient BBU addition/upgrade compared to traditional RAN [5,6]. To benefit from network function virtualization (NFV) [7], we adopt the case of virtualized

BBU computational resources (V-BBU) connected to the RRHs assuming a large capacity and low-latency fronthaul, under the common public radio interface (CPRI) [8].

Various important C-RAN architectural aspects have been studied during the last years, including (a) capacity demands and possible functional splits of the fronthaul network [9–11], (b) security and/or privacy challenges [12,13], (c) cost and/or energy-saving issues [14–17], and (d) network slicing issues [18–20]. At the same time, very few papers exist in the literature (to the best of our knowledge) that investigate call admission control (CAC) and propose efficient formulas for the call blocking probabilities (CBP) computation [21–28]. Such CBP formulas are always desirable by telecom companies as they are not computationally complex and therefore can be considered when networks should be dimensioned.

In [21], a cluster of RRHs is studied where all RRHs have the same RRUs capacity. Calls have the same resource requirements and therefore they form a single service class while their arrival process in the RRHs is Poisson. More specifically, a call requires two different resource units (RUs): a computational one (we name it CRU) from the V-BBU and a RRU from the (serving) RRH. If these RUs are available, then the call is serviced for a service time which can be generally distributed. Otherwise, the call is blocked and lost. This single-class-single-cluster (SC-SC) model has a product form solution (PFS) which is essential for the accurate (compared to simulation) CBP computation. The SC-SC model has been extended in [22,23] to include the case of overlapping cells and in [24] to include the case of grouping the RRHs in many clusters, according to their RRUs capacity. Due to this particular feature, we name the model proposed in [24], single-class-multi-cluster (SC-MC) model. The SC-SC has been extended in [27] to include the case of RRHs serving quasi-random traffic, i.e., traffic generated by a finite number of MUs. We name the model of [27] finite SC-SC (f-SC-SC). Later, in [25], the SC-SC model was further extended to include the case of RRHs serving a mixture of quasi-random, random, and batched Poisson traffic, where calls arrive in the network as batches which follow a Poisson process [29,30]. The SC-MC model has been extended in [28] to accommodate quasi-random traffic and the model was named f-SC-MC. It was also further extended in [26] to include the case of RRHs serving a mixture of quasi-random, random, and batched Poisson traffic.

The common feature of [21–28] is that all RRHs serve calls which require nothing but a single RRU and CRU (single-service calls). However, in modern networks it is significant to be able to study a multiservice environment where calls need more resources. The analysis at call-level of such contemporary networks is essential in network planning procedures [31–43].

In this paper, a generalization of both the f-SC-SC and f-SC-MC models is proposed by considering that RRHs accommodate different service classes with different (per call) resource requirements. A candidate application is the enhanced mobile broadband case which considers service classes with high resource requirements such as virtual reality and online 4K video [44,45]. The proposed work is the first that studies a C-RAN that accommodates multiservice quasi-random traffic and, at the same time, provides convolution algorithms for the efficient determination of congestion probabilities (recently, the case of C-RAN multi-service random traffic has been proposed in [46]). Such algorithms are used in the literature in order to express complicated resource sharing policies such as the bandwidth reservation policy and threshold-based policies [47–54]. The proposed models of this paper are named finite multi-class-single-cluster (f-MC-SC) and finite multi-class-multi-cluster (f-MC-MC), respectively, while the summary of our contribution is as follows: (1) we propose the f-MC-SC model and show that the model has a PFS, (2) we present a brute force (BF) analytical method together with a convolution algorithm for the calculation of congestion probabilities in the proposed model, (3) we compare the congestion probabilities results of the f-MC-SC model with simulation results and those obtained via [27], (4) we propose the f-MC-MC model and show that the model has a PFS, and (5) we present a BF method as well as a convolution algorithm for the determination of congestion probabilities in the f-MC-MC model.

The remainder of this paper is as follows. In Section 2, we propose the f-MC-SC model. In Section 2.1, we determine the steady-state probabilities of the proposed model via a PFS, while in Sections 2.2 and 2.3, we propose a BF method as well as a convolution algorithm for the determination of congestion probabilities, respectively. In Section 3, we provide simulation and analytical congestion probabilities results for the proposed f-MC-SC model and analytical congestion probabilities results of the f-SC-SC model of [27]. In Section 4, we propose the f-MC-MC model. In Section 4.1, we determine show that the model has PFS, while in Sections 4.2 and 4.3, we propose a BF method and a convolution algorithm for the computation of congestion probabilities, respectively. We conclude in Section 5.

A list of abbreviations is presented in Table 1.

Table 1. Abbreviations list.

BBU	Baseband units
BF	Brute force
CAC	Call admission control
CBP	Call blocking probabilities
CC	Call congestion
CPRI	Common public radio interface
C-RAN	Cloud radio access network
CRUs	Computational resource units
f-MC-MC	Finite multi-class-multi-cluster
f-MC-SC	Finite multi-class-single-cluster
f-SC-MC	Finite single-class-multi-cluster
f-SC-SC	Finite single-class-single-cluster
MUs	Mobile users
NFV	Network function virtualization
PFS	Product form solution
o.d.	Occupancy distribution
QoE	Quality of experience
QoS	Quality of service
RRH	Remote radio head
RRUs	Radio resource units
RUs	Resource units
TC	Time congestion
V-BBU	Virtualized BBU

2. The f-MC-SC Model

2.1. The Analytical Model

Consider Figure 1 which presents the adopted C-RAN architecture where the centralized V-BBU and the RRHs are separated. There are W RRHs of capacity C RRUs which form a single cluster, justifying the abbreviation SC in the name of the model. The V-BBU can provide T CRUs to those calls that will be accepted in the system under consideration. The w-th RRH ($w = 1, \ldots, W$) accommodates calls that may have different RUs requirements. Calls with the same RUs requirements are grouped in the same service class. Thus, calls arriving to the w-th RRH are grouped into S_w service classes.

A call of service class s ($s = 1, \ldots, S_w$) arrives to the w-th RRH according to a quasi-random process with arrival rate $\lambda_{w,s} = (N_{w,s} - n_{w,s})v_{w,s}$, where $N_{w,s}$ is the finite population of MUs, that use service class s and can be served by the w-th RRH, $n_{w,s}$ is the number of in-service calls of service class s calls in the w-th RRH, and $v_{w,s}$ is the mean call arrival rate per idle MU of service class s in the w-th RRH.

An incoming call of service class s that arrives to the w-th RRH requires $b^{\mathrm{r}}_{w,s}$ RRUs and $b^{\mathrm{c}}_{w,s}$ CRUs, and we assume that $b^{\mathrm{r}}_{w,s} = b^{\mathrm{c}}_{w,s} \in \mathbb{N}$. For the w-th RRH to accept an arriving service class s call, the CAC consists of two conditions: one stating that there should be enough spare RRUs in the (serving) w-th RRH, and the other stating that there should be enough spare CRUs in the V-BBU. That is, the w-th RRH accepts an incoming service class s call if the occupied RRUs are not more than $C - b^{\mathrm{r}}_{w,s}$ and the occupied CRUs in the V-BBU are not more than $T - b^{\mathrm{c}}_{w,s}$. If the incoming call is accepted, it remains in the w-th RRH for a generally distributed service time with mean value $\mu^{-1}_{w,s}$. In the opposite case, the call is blocked and lost.

Having defined the service time of a call, the offered traffic load per idle service class s MU (in erl), in the w-th RRH, is $\alpha_{w,s,\mathrm{idle}} = v_{w,s}/\mu_{w,s}$.

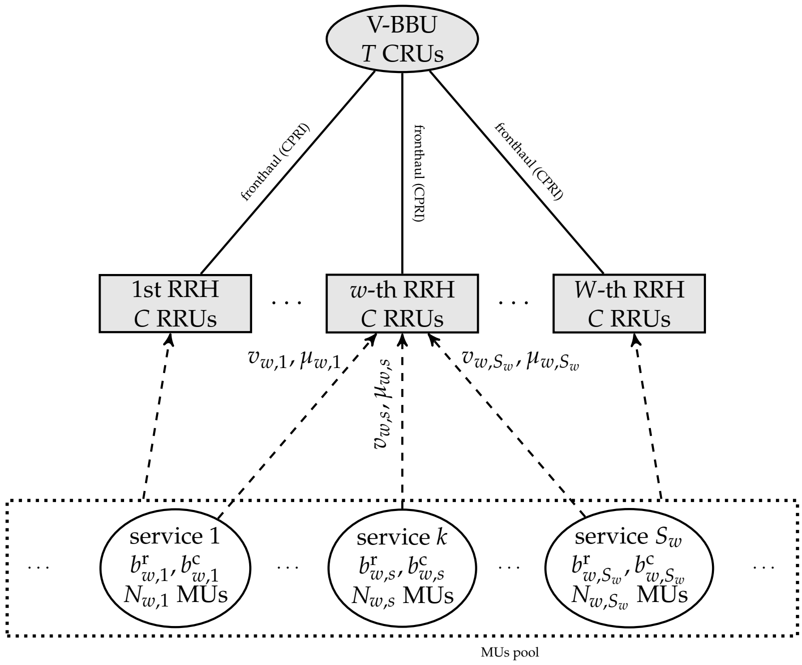

Figure 1. The f-MC-SC model.

Let $n_{w,s} \geq 0$ be the in-service service class s calls in the w-th RRH. Then, the steady-state vector $\boldsymbol{n} = (n_{1,1}, \ldots, n_{1,S_1}, \ldots, n_{w,1}, \ldots, n_{w,s}, \ldots, n_{w,S_w}, \ldots, n_{W,1}, \ldots, n_{W,S_W})$ expresses all in-service calls of all service classes in the system. The system's state space, $\boldsymbol{\Omega}$, expresses all possible states and can be described via:

$$\boldsymbol{\Omega} = \left\{ \boldsymbol{n} : n_{w,s} \geq 0, \sum_{s=1}^{S_w} n_{w,s} b^{\mathrm{r}}_{w,s} \leq C, \sum_{w=1}^{W} \sum_{s=1}^{S_w} n_{w,s} b^{\mathrm{c}}_{w,s} \leq T \right\}. \tag{1}$$

To determine the probability the system is in steady-state $\boldsymbol{n}$, $P_{\mathrm{fin}}(\boldsymbol{n})$, it is necessary to define the adjacent vectors $\boldsymbol{n}^-_{w,s} = (n_{1,1}, \ldots, n_{1,S_1}, \ldots, n_{w,1}, \ldots, n_{w,s} - 1, \ldots, n_{w,S_w}, \ldots, n_{W,1}, \ldots, n_{W,S_W})$ and $\boldsymbol{n}^+_{w,s} = (n_{1,1}, \ldots, n_{1,S_1}, \ldots, n_{w,1}, \ldots, n_{w,s} + 1, \ldots, n_{w,S_w}, \ldots, n_{W,1}, \ldots, n_{W,S_W})$ as well as the corresponding steady-state probability distributions $P_{\mathrm{fin}}(\boldsymbol{n}^-_{w,s})$ and $P_{\mathrm{fin}}(\boldsymbol{n}^+_{w,s})$, respectively.

Assuming that $\boldsymbol{n}^-_{w,s}, \boldsymbol{n}, \boldsymbol{n}^+_{w,s} \in \boldsymbol{\Omega}$, Figure 2 presents the corresponding state transition diagram for service class s calls in the (serving) w-th RRH.

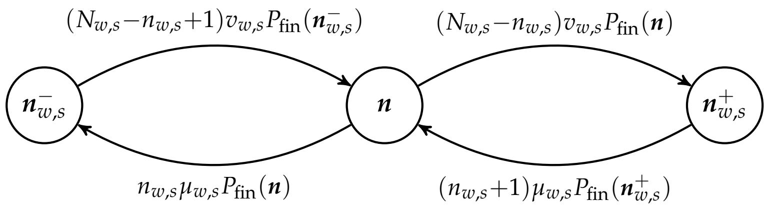

Figure 2. Transition diagram for calls of service class s in the w-th RRH.

Based on Figure 2 and the reversibility of the corresponding Markov chain, we have a local balance equation, for the adjacent states $\boldsymbol{n}_{w,s}^{-}$ and $\boldsymbol{n}$:

$$(N_{w,s} - n_{w,s} + 1) v_{w,s} P_{\text{fin}}(\boldsymbol{n}_{w,s}^{-}) = n_{w,s} \mu_{w,s} P_{\text{fin}}(\boldsymbol{n}) \tag{2}$$

and an additional one for states $\boldsymbol{n}$ and $\boldsymbol{n}_{w,s}^{+}$:

$$(N_{w,s} - n_{w,s}) v_{w,s} P_{\text{fin}}(\boldsymbol{n}) = (n_{w,s} + 1) \mu_{w,s} P_{\text{fin}}(\boldsymbol{n}_{w,s}^{+}). \tag{3}$$

Equations (2) and (3) are satisfied by the PFS according to (4), when $\boldsymbol{n} \in \boldsymbol{\Omega}$:

$$P_{\text{fin}}(\boldsymbol{n}) = \frac{1}{G} \prod_{w=1}^{W} \prod_{s=1}^{S_w} \binom{N_{w,s}}{n_{w,s}} \alpha_{w,s,\text{idle}}^{n_{w,s}}, \tag{4}$$

where $G = \sum_{\boldsymbol{n} \in \boldsymbol{\Omega}} \prod_{w=1}^{W} \prod_{s=1}^{S_w} \binom{N_{w,s}}{n_{w,s}} \alpha_{w,s,\text{idle}}^{n_{w,s}}$ refers to the normalization constant.

In a system that accommodates calls generated via a finite number of traffic sources (users), we distinguish CBP in time congestion (TC) and call congestion (CC) probabilities. The latter refers to CBP, while the former refers to the proportion of time the system is under congestion. Assuming that the number of traffic sources (i.e., the number of MUs) is high, then CC probabilities are slightly lower than TC probabilities in quasi-random single or multi-rate loss models [29,30]. Assuming Poisson arrivals and taking into consideration the PASTA property [29,30], it is easy to verify that TC and CC probabilities lead to the same results. The total TC probability for the service class w,s calls, $B_{\text{tot},w,s}^{\text{TC}}$, can be calculated via:

$$B_{\text{tot},w,s}^{\text{TC}} = B_{\text{r},w,s}^{\text{TC}} + B_{\text{c},w,s}^{\text{TC}} \tag{5}$$

where $B_{\text{r},w,s}^{\text{TC}}$, $B_{\text{c},w,s}^{\text{TC}}$ are the TC probabilities caused as the result of insufficient RRUs and CRUs for the service class w,s calls, respectively. In order to sum up $B_{\text{r},w,s}^{\text{TC}}$ and $B_{\text{c},w,s}^{\text{TC}}$ the sets of steady-states that form them should be disjoint. When the steady-state has both insufficient CRUs and RRUs, it is accounted only to the $B_{\text{c},w,s}^{\text{TC}}$.

Regarding the CC probabilities for service class s calls, they are determined assuming $N_{w,s} - 1$ sources.

The values of $B_{\text{tot},w,s}^{\text{TC}}$ can be computed using either a BF method or a convolution algorithm (which are described in Sections 2.2 and 2.3, respectively).

2.2. TC Probabilities via the Proposed BF Method

Let us define the set of steady-states, $\boldsymbol{\Omega}_{w,s}^{C,<T}$, in which there are no more RRUs in the w-th RRH for service class s calls, excluding those states in which there are also no CRUs left in V-BBU for the same service class calls. This set can be written as $\boldsymbol{\Omega}_{w,s}^{C,<T} = \{\boldsymbol{\Omega}_{w,s}^{C} \cap \boldsymbol{\Omega}_{w,s}^{<T}\}$ with $\boldsymbol{\Omega}_{w,s}^{C} = \{\boldsymbol{n} : C - b_{w,s}^{\text{r}} < \sum_{y=1}^{S_w} n_{w,y} b_{w,y}^{\text{r}} \leq C\}$ and $\boldsymbol{\Omega}_{w,s}^{<T} = \{\boldsymbol{n} : \sum_{x=1}^{W} \sum_{y=1}^{S_x} n_{x,y} b_{x,y}^{\text{c}} \leq T - b_{w,s}^{\text{c}}\}$. Then, the values of $B_{\text{r},w,s}^{\text{TC}}$ can be computed (using PFS (4)) as follows:

$$B_{\text{r},w,s}^{\text{TC}} = \sum_{\boldsymbol{n} \in \boldsymbol{\Omega}_{w,s}^{C,<T}} P_{\text{fin}}(\boldsymbol{n}). \tag{6}$$

Similarly, by considering $\boldsymbol{\Omega}_{w,s}^{T} = \{\boldsymbol{n} : T - b_{w,s}^{\text{c}} < \sum_{x=1}^{W} \sum_{y=1}^{S_x} n_{x,y} b_{x,y}^{\text{c}} \leq T\}$ as the set of steady-states in which there are no CRUs left in the V-BBU for the service class w,s calls, the values of $B_{\text{c},w,s}^{\text{TC}}$, can be computed via:

$$B_{\text{c},w,s}^{\text{TC}} = \sum_{\boldsymbol{n} \in \boldsymbol{\Omega}_{w,s}^{T}} P_{\text{fin}}(\boldsymbol{n}). \tag{7}$$

Note that the set $\boldsymbol{\Omega}_{w,s}^{T}$ includes states that lead to TC due to the unavailability of CRUs, as well as due to both insufficient CRUs and RRUs.

Computing $B^{\mathrm{TC}}_{\mathrm{r},w,s}$ and $B^{\mathrm{TC}}_{\mathrm{c},w,s}$ is accurate (if one compares the analytical results with the corresponding simulation results) but complex especially for a system of many RRHs that have large capacities and serve many service classes. This is because it is required to enumerate/process $\mathbf{\Omega}$ so as to compute the normalization constant G of (4) and determine all blocking states required in (6) and (7). For this reason, the BF method can be adopted only for small C-RAN examples (of tutorial nature). To circumvent this problem, in the next subsection we propose a convolution algorithm that leads to an efficient determination of the TC probabilities.

2.3. TC Probabilities via the Proposed Convolution Algorithm

The algorithm of this section consists of three steps (presented below as steps A to C) and takes advantage of the fact that the analytical model has a PFS.

Step A

In this step, the occupancy distribution (o.d.) of the RRHs is calculated. To this end, we first calculate the o.d. for each service class w,s calls, $q_{\mathrm{f},w,s}(j)$, assuming that the w-th RRH serves only service class s calls:

$$q_{\mathrm{f},w,s}(j) = \begin{cases} 1, & \text{for } j = 0 \\ \binom{N_{w,s}}{i}\alpha^{i}_{w,s,\mathrm{idle}} q_{\mathrm{f},w,s}(0), & \text{for } 1 \leq i \leq \lfloor \frac{C}{b^{\mathrm{r}}_{w,s}} \rfloor, j{=}ib^{\mathrm{r}}_{w,s}, \\ 0, & \text{otherwise} \end{cases} \tag{8}$$

where i expresses the number of in-service service class s calls while j expresses the occupied RRUs. The values of $q_{\mathrm{f},w,s}(j)$ are normalized via $G_{\mathrm{f},w,s} = \sum_{j=0}^{C} q_{\mathrm{f},w,s}(j)$ and are denoted as $q'_{\mathrm{f},w,s}(j) = q_{\mathrm{f},w,s}(j)/G_{\mathrm{f},w,s}$.

Having determined $q'_{\mathrm{f},w,s}(j)$, one should calculate, without considering the first service class, the aggregated o.d. of the w-th RRH $Q^{w}_{\mathrm{f},(-1)}$:

$$Q^{w}_{\mathrm{f},(-1)} = q'_{\mathrm{f},w,2} * \ldots * q'_{\mathrm{f},w,s} * \ldots * q'_{\mathrm{f},w,S_w}, \tag{9}$$

where the convolution operation between $q'_{\mathrm{f},w,x} \equiv q'_{\mathrm{f},a}$ and $q'_{\mathrm{f},w,y} \equiv q'_{\mathrm{f},b}$ can be expressed via:

$$q'_{\mathrm{f},a} * q'_{\mathrm{f},b} = \left\{ q'_{\mathrm{f},a}(0) \cdot q'_{\mathrm{f},b}(0), \sum_{i=0}^{1} q'_{\mathrm{f},a}(i) \cdot q'_{\mathrm{f},b}(1-i), \ldots, \sum_{i=0}^{C} q'_{\mathrm{f},a}(i) \cdot q'_{\mathrm{f},b}(C-i) \right\}. \tag{10}$$

Finally, to compute the normalized o.d. of the w-th RRH, $q'_{\mathrm{f},w}$, one should compute $q_{\mathrm{f},w} = Q^{w}_{\mathrm{f},(-1)} * q'_{\mathrm{f},w,1}$ as well as the normalization $q'_{\mathrm{f},w}(j) = q_{\mathrm{f},w}(j)/G_{\mathrm{f},w}$ where $G_{\mathrm{f},w} = \sum_{j=0}^{C} q_{\mathrm{f},w}(j)$.

Step B

Herein, we compute, for all RRHs, the aggregated o.d. excluding the w-th one, via:

$$Q_{\mathrm{f},(-w)} = q'_{\mathrm{f},1} * \ldots * q'_{\mathrm{f},w-1} * q'_{\mathrm{f},w+1} * \ldots * q'_{\mathrm{f},W}. \tag{11}$$

The convolution operation between $q'_{\mathrm{f},x}$ and $q'_{\mathrm{f},y}$ is the following:

$$q'_{\mathrm{f},x} * q'_{\mathrm{f},y} = \left\{ q'_{\mathrm{f},x}(0) \cdot q'_{\mathrm{f},y}(0), \sum_{i=0}^{1} q'_{\mathrm{f},x}(i) \cdot q'_{\mathrm{f},y}(1-i), \ldots, \sum_{i=0}^{T} q'_{\mathrm{f},x}(i) \cdot q'_{\mathrm{f},y}(T-i) \right\}. \tag{12}$$

The normalized values of $Q_{\mathrm{f},(-w)}(j)$, expressed according to the notation $Q'_{\mathrm{f},(-w)}(j)$, are determined via $Q'_{\mathrm{f},(-w)}(j) = Q_{\mathrm{f},(-w)}(j)/G_{\mathrm{f},(-w)}$, where $G_{\mathrm{f},(-w)} = \sum_{j=0}^{T} Q_{\mathrm{f},(-w)}(j)$.

Step C

In this step, we consider the operation $Q'_{\mathrm{f},(-w)} * q'_{\mathrm{f},w}$ which results to the un-normalized values of $Q_{\mathrm{f},w}(j)$ which can be normalized via $G^*_{\mathrm{f},w} = \sum_{j=0}^{T} Q_{\mathrm{f},w}(j)$:

$$Q'_{\mathrm{f}}(j) = \frac{Q_{\mathrm{f},w}(j)}{G^*_{\mathrm{f},w}}. \tag{13}$$

To obtain the computational o.d. $Q'_{\mathrm{f}}(j)$, one may choose any of the W RRHs since all RRHs are exactly the same.

Based on (13), we calculate the TC probabilities due to the unavailability of CRUs and RRUs according to (14) and (15), respectively:

$$B^{\mathrm{TC}}_{\mathrm{c},w,s} = \sum_{j=T-b^{\mathrm{c}}_{w,s}+1}^{T} Q'_{\mathrm{f}}(j), \tag{14}$$

$$B^{\mathrm{TC}}_{\mathrm{r},w,s} = \frac{1}{G^*_{\mathrm{f},w}} \sum_{x=C-b^{\mathrm{r}}_{w,s}+1}^{C} q'_{\mathrm{f},w}(x) \sum_{y=x}^{T-b^{\mathrm{r}}_{w,s}} Q'_{\mathrm{f},(-w)}(T - b^{\mathrm{r}}_{w,s} - y). \tag{15}$$

3. Evaluation

In this section, we present a C-RAN example and provide simulation and analytical TC probabilities for the f-MC-SC model together with the corresponding analytical TC probabilities results for the f-SC-SC model of [27]. The simulation values presented in this example are based on SIMSCRIPT III [55] and are the mean values of seven runs. In every run (which took around 3 min of simulation time in a computer of Intel(R) Core(TM) i5-2430M CPU @ 2.4 GHz and 4 GB RAM), two hundred million calls are generated while the initial 5% of them is not taken into consideration in the TC probabilities so as to have a warm-up period [56,57].

In the C-RAN example, let $W = 6$ RRHs of $C = 10$ RRUs. Furthermore, let $T = 30$ CRUs. The w-th RRH ($w = 1, \ldots, 6$) serves S_w service classes and let $b_{w,s} = b^{\mathrm{c}}_{w,s} = b^{\mathrm{r}}_{w,s}$ be the RUs required by a service class s call (which is going to be serviced in the w-th RRH). To be more specific, the first RRH accommodates $S_1 = 3$ service classes. First service class calls require $b_{1,1} = 1$ RU, second service class calls require $b_{1,2} = 2$ RUs while third service class calls require $b_{1,3} = 3$ RUs. On the same hand, the second RRH accommodates $S_2 = 2$ service classes, with $b_{2,1} = 2$ RUs and $b_{2,2} = 3$ RUs. Similarly, the third RRH accommodates $S_3 = 2$ service classes, with $b_{3,1} = 1$ RU and $b_{3,2} = 3$ RUs; the fourth RRH accommodates $S_4 = 2$ service classes, with $b_{4,1} = 1$ RU and $b_{4,2} = 2$ RUs; the fifth RRH accommodates a single service class with $b_{5,1} = 2$ RUs; and the sixth RRH accommodates a service class with $b_{6,1} = 1$ RU. Regarding the number of finite sources (i.e., MUs) that generate traffic, we assume that $N_{w,s} = 10$. As far as the offered traffic-load is concerned, we initially consider that $\alpha_{w,s} = \alpha_{w,s,\mathrm{idle}} N_{w,s} = 1$ erl for all service classes in all RRHs (which refers to point 1 in the x-axis of Figures 3–9). We evaluate the C-RAN, by calculating the TC probabilities for 31 steps, where a 0.2 offered traffic-load increase per step is considered. Because of this, in the last step (point 31 in the x-axis of Figures 3–9) we have $\alpha_{w,s} = 7$ erl.

For comparison, we study the f-SC-SC model of [27] where calls require a single RU for their connection in the system, while the number of RRHs, as well as the radio and computational capacity (in RUs) are exactly the same with those given above. Furthermore, all RRHs have a finite population of MUs equal to $N_w = 10$. As the model of [27] is a single service class model, we should express, for every RRH, the offered traffic-load α_w. Because of this, we adopt a load factor l_w, expressed via $l_w = \sum_{s=1}^{S_w} b_{w,s}$ where S_w and $b_{w,s}$ are the values of the proposed f-MC-SC model, while $w = 1, \ldots, 6$. The initial values of α_w are the same with those of l_w, i.e.,: $(\alpha_1, \alpha_2, \alpha_3, \alpha_4, \alpha_5, \alpha_6) = (6, 5, 4, 3, 2, 1)$. Again, 31 steps are taken into consideration where α_m increases by $0.2 l_w$ in each step. Thus, in the last step, the offered traffic-load values are $(\alpha_1, \alpha_2, \alpha_3, \alpha_4, \alpha_5, \alpha_6) = (42, 35, 28, 21, 14, 7)$.

Furthermore, note that in Figures 3–9 (a) we do not present the index "TC" in the graphical representation of the TC probabilities so as to increase the readability of these figures and (b) the analytical results are represented with different types of lines, while the simulation results are represented with different types of dots.

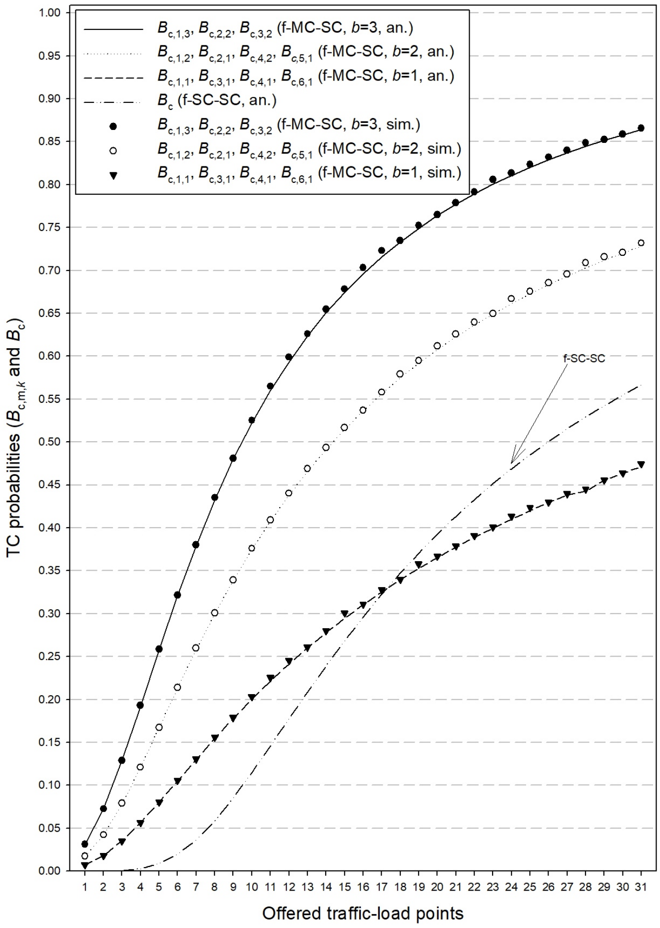

Figure 3. TC probabilities due to lack of CRUs.

In Figure 3, we present the analytical and simulation TC probabilities results due to the unavailability of CRUs ($B_{c,w,s}^{TC}$) of the f-MC-SC model and the corresponding (analytical) TC probabilities results (B_c^{TC}) of the f-SC-SC model. According to Figure 3, we conclude that (a) simulation and analytical TC probabilities results are almost identical, (b) the offered traffic-load increase leads to an increase of TC probabilities, and (c) the f-SC-SC model cannot behave similar to the f-MC-SC model because of the fact that the former refers to a single service class model.

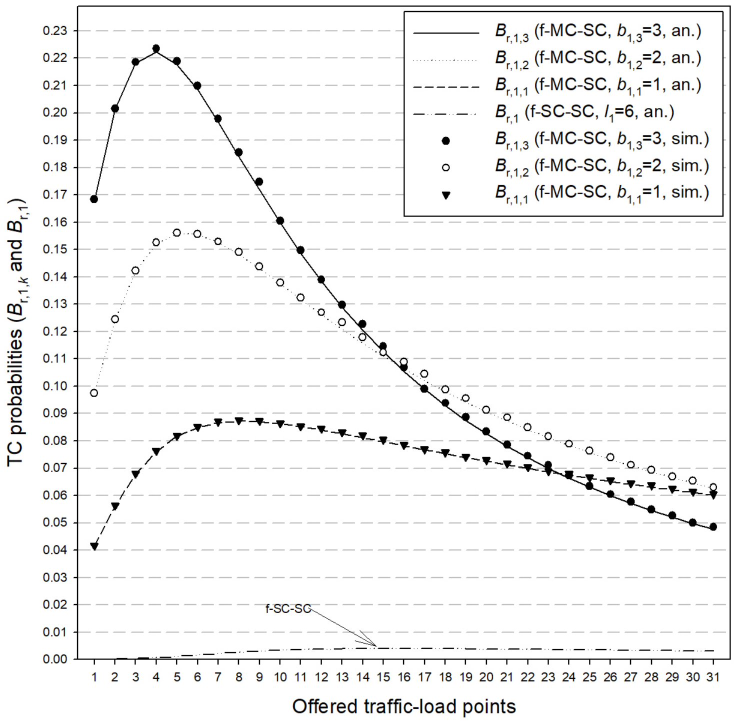

Figure 4. TC probabilities due to RRUs unavailability (1st RRH).

In Figures 4–6, we present TC probabilities results for the 1st, 2nd, and 3rd RRH, respectively. More precisely, in Figure 4, we show the simulation and analytical TC probabilities results of $B_{r,1,s}^{TC}$ for the three service classes of the f-MC-SC model and the corresponding analytical TC probabilities results for the f-SC-SC model. In the case of the f-SC-SC model, the first point in the x-axis of Figure 4 expresses the value of $\alpha_1 = 6$ erl, while the last point (i.e., point 31) expresses the value of $\alpha_1 = 42$ erl. Similarly, in Figure 5, we show the simulation and analytical TC probabilities results of $B_{r,2,s}^{TC}$ for the two service classes of the f-MC-SC model and the corresponding analytical TC probabilities results for the f-SC-SC model. In the case of the f-SC-SC model, the first point in Figure 5 expresses the value of $\alpha_2 = 5$ erl, while the last point (i.e., point 31) expresses the value of $\alpha_2 = 35$ erl. Finally, in Figure 6, the third RRH is considered and we present the simulation and analytical TC probabilities results of $B_{r,3,s}^{TC}$ for the two service classes of the f-MC-SC model and the corresponding analytical TC probabilities results for the f-SC-SC model. In the case of the f-SC-SC model, the first point in the x-axis of Figure 6 expresses the value of $\alpha_3 = 4$ erl while the last point (i.e., point 31) expresses the value of $\alpha_3 = 28$ erl. Based on Figures 4–6, we observe that (a) simulation and analytical TC probabilities results are almost identical in the f-MC-SC model which is expected as the proposed model has a PFS, (b) the TC probabilities results obtained via the f-SC-SC model cannot capture the behaviour of the f-MC-SC model, and (c) the TC probabilities results (because of the RRUs unavailability) increase as the offered traffic load increases but after a point (which is not easy to know it in advance) they decrease. This behaviour is justified by observing that the TC probabilities results due to the unavailability of CRUs (see Figure 3), increase when the traffic load becomes higher and thus more RRUs remain intact in the corresponding RRHs. A similar behaviour (a decrease in congestion probabilities, after a certain point, when the offered traffic load increases) has been observed in the past when studying classical multi-rate loss models under the complete sharing policy and the bandwidth reservation policy, particularly when two service classes are considered and the required RUs of each service class have a high difference [58,59]. Under these conditions, congestion probabilities oscillations may occur and therefore it remains an open issue to study if such type of oscillations may occur in a multiservice C-RAN environment.

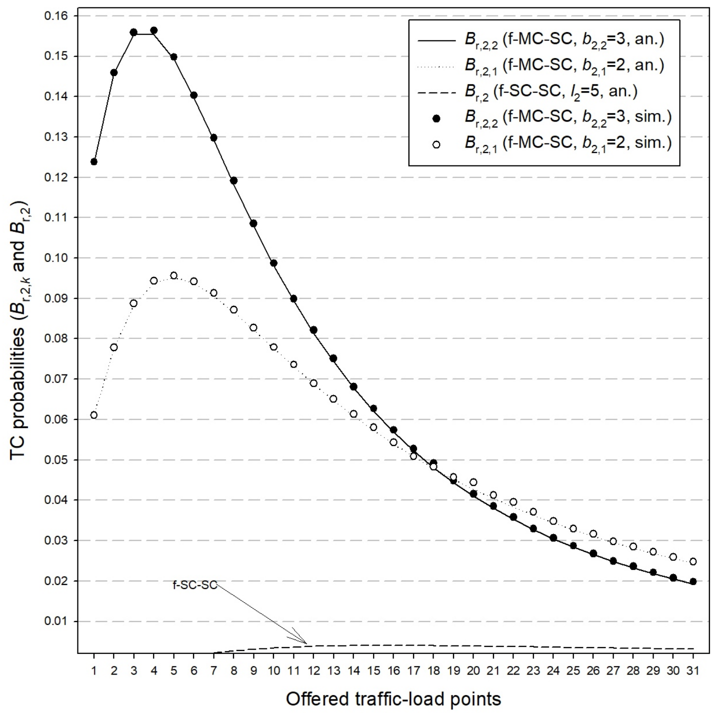

Figure 5. TC probabilities as the result of RRUs unavailability (2nd RRH).

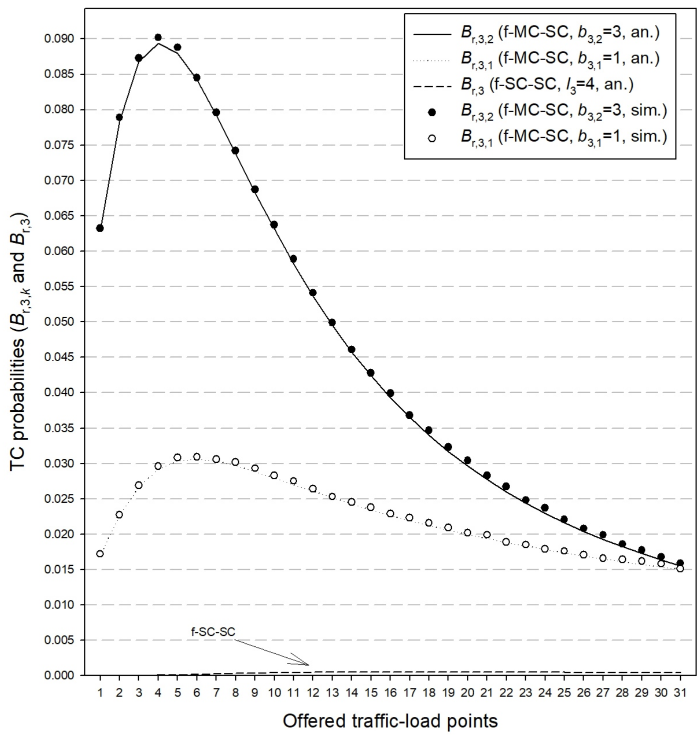

Figure 6. TC probabilities as the result of RRUs unavailability (3rd RRH).

In Figures 7–9, we study again the 1st, 2nd, and 3rd RRH, respectively, and present the total TC probabilities (computed via (5) as well as (14), (15)). Based on Figures 7–9, we conclude that (a) simulation and analytical results are again almost identical, (b) the increase of offered traffic-load increases the corresponding total TC probabilities, and (c) the f-SC-SC model cannot behave similar to the proposed model.

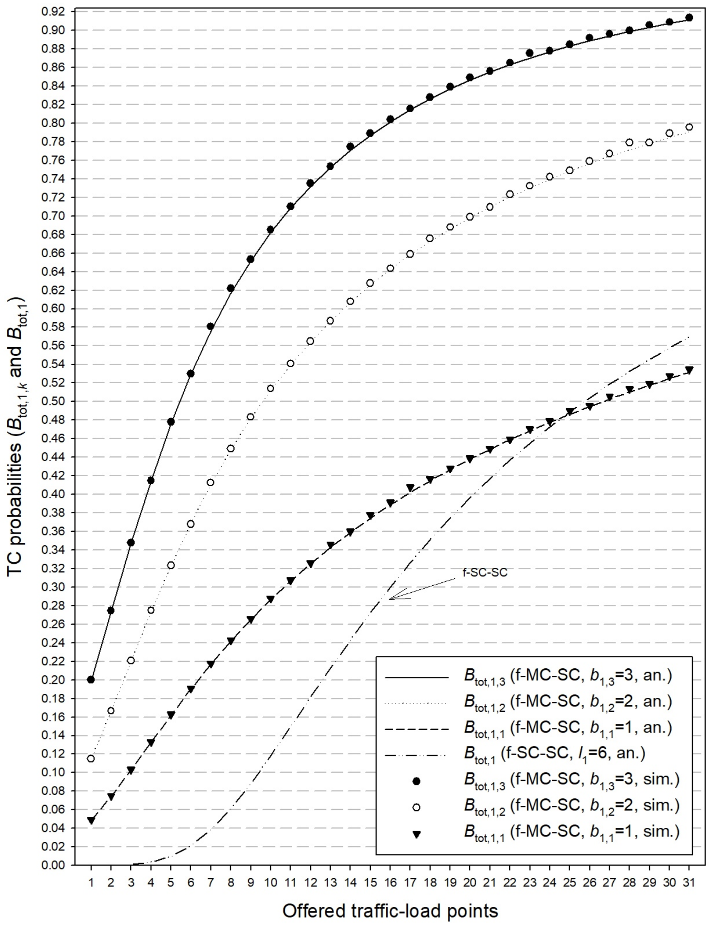

Figure 7. Total TC probabilities (1st RRH—all service classes).

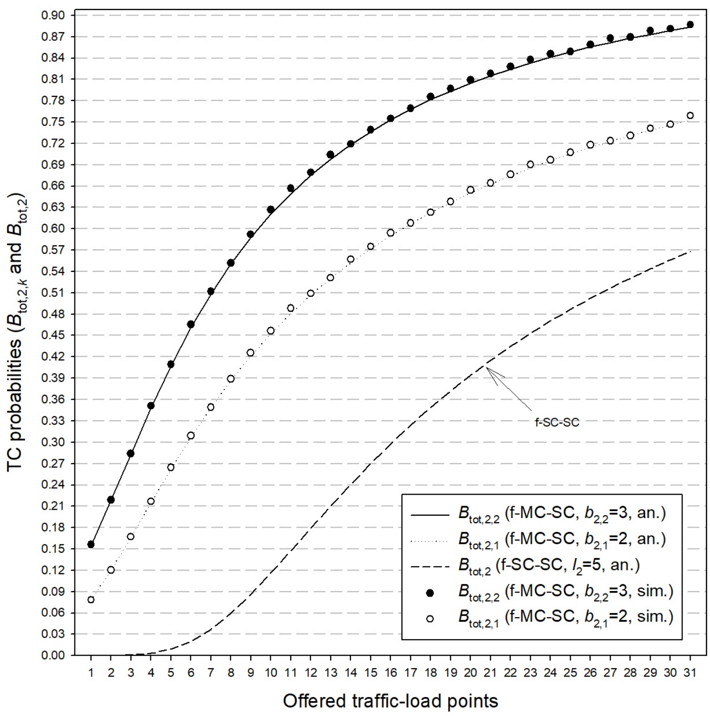

Figure 8. Total TC probabilities (2nd RRH—all service classes).

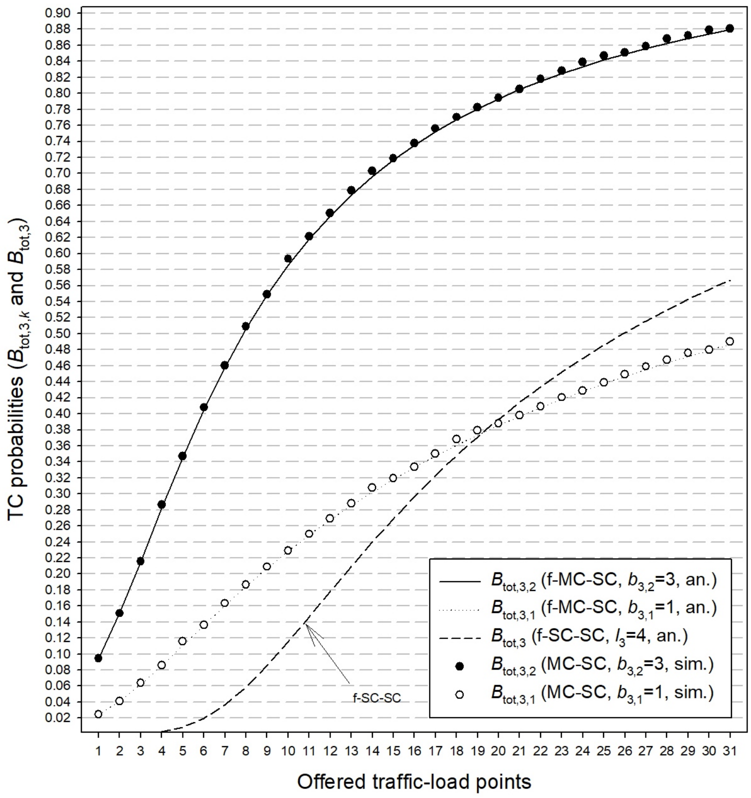

Figure 9. Total TC probabilities (3rd RRH—all service classes).

4. The Generalized f-MC-MC Model

In this section, we present the f-MC-MC model which generalizes the f-MC-SC model by taking into consideration the grouping of RRHs in different clusters based on their RRUs capacity, thus forming a multi-cluster of RRHs.

4.1. The Analytical Model

Consider Figure 10 where U clusters of RRHs are presented and are separated from the V-BBU whose capacity remains the same as in the f-MC-SC model (i.e., T CRUs). Cluster u ($u = 1, \ldots, U$) consists of W_u RRHs. Each of these RRHs has capacity of C_u RRUs.

The w-th RRH of cluster u ($w = 1, \ldots, W_u$) accommodates calls from $S_{u,w}$ different service classes. A call of service class s ($s = 1, \ldots, S_{u,w}$) arrives to the u, w-th RRH according to a quasi-random process with arrival rate $\lambda_{u,w,s} = (N_{u,w,s} - n_{u,w,s})v_{u,w,s}$, where $N_{u,w,s}$ is the population of MUs, $n_{u,w,s}$ is the in-service calls of service class s calls in the u, w-th RRH, and $v_{u,w,s}$ is the call arrival rate per idle MU of service class s in the u, w-th RRH. A call of service class u, w, s requires $b^{r}_{u,w,s}$ RRUs and $b^{c}_{u,w,s}$ CRUs, assuming that $b^{r}_{u,w,s} = b^{c}_{u,w,s}$. An accepted call remains in the u, w-th RRH for a service time whose distribution can be general with mean $\mu^{-1}_{u,w,s}$ if the required RUs are available when the call arrives in the serving RRH, i.e., if the occupied RRUs in the u, w-th RRH do not exceed the value of $C_u - b^{r}_{u,w,s}$ and the occupied CRUs are not more than $T - b^{c}_{u,w,s}$. In the opposite case, call blocking occurs.

Let $n_{u,w,s} \geq 0$ be the in-service calls of service class u, w, s ($u = 1, \ldots, U$, $w = 1, \ldots, W_u$, $s = 1, \ldots, S_{u,w}$). Then, we can denote both the vector $\boldsymbol{n} = (n_{1,1,1}, \ldots, n_{1,1,S_{1,1}}, \ldots, n_{u,w,1}, \ldots, n_{u,w,s}, \ldots, n_{u,w,S_{u,w}}, \ldots, n_{U,W_U,1}, \ldots, n_{U,W_U,S_{U,W_U}})$ and $\boldsymbol{\Omega}$ via:

$$\boldsymbol{\Omega} = \left\{ \boldsymbol{n} : n_{u,w,s} \geq 0, \sum_{s=1}^{S_{u,w}} n_{u,w,s} b^{r}_{u,w,s} \leq C_u, \sum_{u=1}^{U} \sum_{w=1}^{W_u} \sum_{s=1}^{S_{u,w}} n_{u,w,s} b^{c}_{u,w,s} \leq T \right\}. \quad (16)$$

To calculate the steady-state probability distribution $P_{\text{g,fin}}(\boldsymbol{n})$, the following vectors are necessary: $\boldsymbol{n}^{-}_{u,w,s} = (n_{1,1,1}, \ldots, n_{1,1,S_{1,1}}, \ldots, n_{u,w,1}, \ldots, n_{u,w,s} - 1, \ldots, n_{u,w,S_{u,w}}, \ldots, n_{U,W_U,1}, \ldots, n_{U,W_U,S_{U,W_U}})$ and $\boldsymbol{n}^{+}_{u,w,s} = (n_{1,1,1}, \ldots, n_{1,1,S_{1,1}}, \ldots, n_{u,w,1}, \ldots, n_{u,w,s} + 1, \ldots, n_{u,w,S_{u,w}}, \ldots, n_{U,W_U,1}, \ldots, n_{U,W_U,S_{U,W_U}})$. Furthermore, let $P_{\text{g,fin}}(\boldsymbol{n}^{-}_{u,w,s})$, $P_{\text{g,fin}}(\boldsymbol{n}^{+}_{u,w,s})$ be the corresponding probability distributions. By further considering that $\boldsymbol{n}^{-}_{u,w,s}, \boldsymbol{n}, \boldsymbol{n}^{+}_{u,w,s}$ belong to $\boldsymbol{\Omega}$, Figure 11 presents the state transition diagram for calls of service class s in the u, w-th RRH.

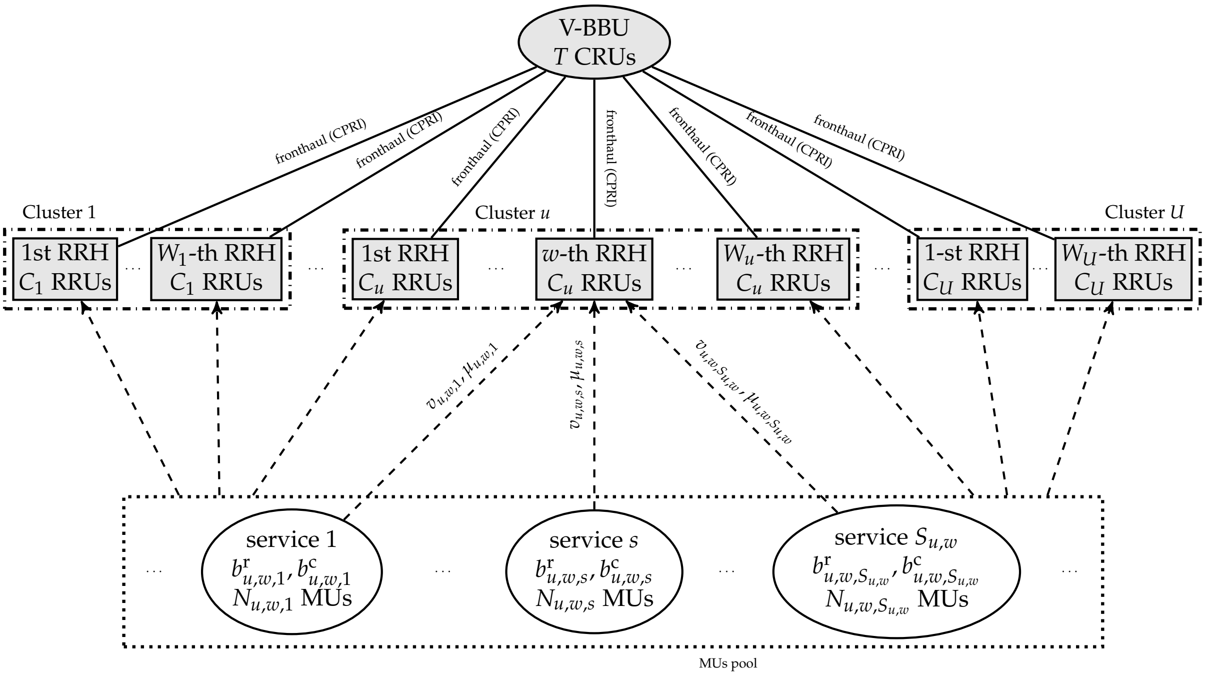

Figure 10. The generalized f-MC-MC model.

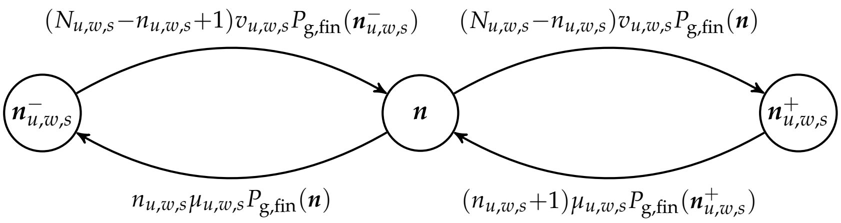

Figure 11. Transition diagram for calls of service class s in the u, w-th RRH.

According to Figure 11 and due to the fact that the Markov chain for service class u, w, s calls is reversible, we have the following local balance equations, for the adjacent states (a) $\boldsymbol{n}^{-}_{u,w,s}$ and $\boldsymbol{n}$ (see (17)) and (b) $\boldsymbol{n}$ and $\boldsymbol{n}^{+}_{u,w,s}$ (see (18)):

$$(N_{u,w,s} - n_{u,w,s} + 1) v_{u,w,s} P_{\text{g,fin}}(\boldsymbol{n}^{-}_{u,w,s}) = n_{u,w,s} \mu_{u,w,s} P_{\text{g,fin}}(\boldsymbol{n}) \quad (17)$$

$$(N_{u,w,s} - n_{u,w,s}) v_{u,w,s} P_{\text{g,fin}}(\boldsymbol{n}) = (n_{u,w,s} + 1) \mu_{u,w,s} P_{\text{g,fin}}(\boldsymbol{n}^{+}_{u,w,s}). \quad (18)$$

The PFS of (19) satisfies both (17) and (18) for $\boldsymbol{n} \in \boldsymbol{\Omega}$:

$$P_{\text{g,fin}}(\boldsymbol{n}) = \frac{1}{G} \prod_{u=1}^{U} \prod_{w=1}^{W_u} \prod_{s=1}^{S_{u,w}} \binom{N_{u,w,s}}{n_{u,w,s}} \alpha_{u,w,s,\text{idle}}^{n_{u,w,s}}, \quad (19)$$

where $G = \sum_{\boldsymbol{n} \in \boldsymbol{\Omega}} \prod_{u=1}^{U} \prod_{w=1}^{W_u} \prod_{s=1}^{S_{u,w}} \binom{N_{u,w,s}}{n_{u,w,s}} \alpha_{u,w,s,\text{idle}}^{n_{u,w,s}}$ and $\alpha_{u,w,s,\text{idle}} = v_{u,w,s} / \mu_{u,w,s}$ is the offered traffic-load per idle MU for the u, w, s service class calls.

Based on (19), we can compute the TC probabilities of service class u, w, s calls: (a) as the result of RRUs unavailability only, $B^{\mathrm{TC}}_{\mathrm{r},u,w,s}$, and (b) as the result of CRUs unavailability, $B^{\mathrm{TC}}_{\mathrm{c},u,w,s}$. Additionally, we can calculate the total TC probability, $B^{\mathrm{TC}}_{\mathrm{tot},u,w,s}$, via:

$$B^{\mathrm{TC}}_{\mathrm{tot},u,w,s} = B^{\mathrm{TC}}_{\mathrm{r},u,w,s} + B^{\mathrm{TC}}_{\mathrm{c},u,w,s}. \tag{20}$$

The values of $B^{\mathrm{TC}}_{\mathrm{tot},u,w,s}$ can be calculated either according to Section 4.2 or according to Section 4.3.

4.2. The BF Method for the Computation of TC Probabilities

The values of $B^{\mathrm{TC}}_{\mathrm{r},u,w,s}$ can be computed, via (21) (using the PFS of (19)):

$$B^{\mathrm{TC}}_{\mathrm{r},u,w,s} = \sum_{\boldsymbol{n} \in \boldsymbol{\Omega}^{C_u,<T}_{u,w,s}} P_{\mathrm{g,fin}}(\boldsymbol{n}), \tag{21}$$

where:

$$\begin{aligned}
\boldsymbol{\Omega}^{C_u,<T}_{u,w,s} &= \{\boldsymbol{\Omega}^{C_u}_{u,w,s} \cap \boldsymbol{\Omega}^{<T}_{u,w,s}\}, \\
\boldsymbol{\Omega}^{C_u}_{u,w,s} &= \{\boldsymbol{n} : C_u - b^{\mathrm{r}}_{u,w,s} < \sum_{z=1}^{S_{u,w}} n_{u,w,z} b^{\mathrm{r}}_{u,w,z} \le C_u\}, \\
\boldsymbol{\Omega}^{<T}_{u,w,s} &= \{\boldsymbol{n} : \sum_{x=1}^{U} \sum_{y=1}^{W_x} \sum_{z=1}^{S_{x,y}} n_{x,y,z} b^{\mathrm{c}}_{x,y,z} \le T - b^{\mathrm{c}}_{u,w,s}\}.
\end{aligned} \tag{22}$$

Similarly, by representing as:

$$\boldsymbol{\Omega}^{T}_{u,w,s} = \{\boldsymbol{n} : T - b^{\mathrm{c}}_{u,w,s} < \sum_{x=1}^{U} \sum_{y=1}^{W_x} \sum_{z=1}^{S_{x,y}} n_{x,y,z} b^{\mathrm{c}}_{x,y,z} \le T\}, \tag{23}$$

we can calculate the TC probabilities of service class u, w, s calls as the result of the CRUs unavailability via:

$$B^{\mathrm{TC}}_{\mathrm{c},u,w,s} = \sum_{\boldsymbol{n} \in \boldsymbol{\Omega}^{T}_{u,w,s}} P_{\mathrm{g,fin}}(\boldsymbol{n}). \tag{24}$$

To avoid the enumeration/processing of $\boldsymbol{\Omega}$ which is mandatory for (21) and (24), we propose a convolution algorithm that leads to the efficient TC probabilities computation.

4.3. The Convolution Algorithm for the Computation of TC Probabilities

The proposed algorithm is based on (19) and can be described as a 3-step algorithm (presented below via steps A to C):

Step A

The target herein, is to compute the o.d. of each RRH. Because of this, we initially calculate the o.d. for each service class s of the u, w-th RRH, $q_{\mathrm{f},u,w,s}(j)$, assuming that the u, w-th RRH services only calls of service class s:

$$q_{\mathrm{f},u,w,s}(j) = \begin{cases} 1, & \text{for } j = 0 \\ \binom{N_{u,w,s}}{i} \alpha^{i}_{u,w,s,\mathrm{idle}} q_{\mathrm{f},u,w,s}(0), & \text{for } 1 \le i \le \lfloor \frac{C_u}{b^{\mathrm{r}}_{u,w,s}} \rfloor, j{=}ib^{\mathrm{r}}_{u,w,s} \,. \\ 0, & \text{otherwise} \end{cases} \tag{25}$$

Note that $q_{\mathrm{f},u,w,s}(j)$ should be normalized via $G_{\mathrm{f},u,w,s}{=}\sum_{j}^{C_u} q_{\mathrm{f},u,w,s}(j)$ and can be denoted as $q'_{\mathrm{f},u,w,s}(j) = q_{\mathrm{f},u,w,s}(j)/G_{\mathrm{f},u,w,s}$.

Having computed $q'_{\mathrm{f},u,w,s}(j)$, we compute the aggregated o.d. of the u,w-th RRH without taking into consideration the first service class, $Q^{u,w}_{\mathrm{f},(-1)}$:

$$Q^{u,w}_{\mathrm{f},(-1)} = q'_{\mathrm{f},u,w,2} * \ldots * q'_{\mathrm{f},u,w,s} * \ldots * q'_{\mathrm{f},u,w,S_{u,w}}, \tag{26}$$

where the operation between $q'_{\mathrm{f},u,w,x} \equiv q'_{\mathrm{f},c}$ and $q_{\mathrm{f},u,w,y} \equiv q'_{\mathrm{f},d}$ takes the following form:

$$q'_{\mathrm{f},c} * q'_{\mathrm{f},d} = \left\{ q'_{\mathrm{f},c}(0) \cdot q'_{\mathrm{f},d}(0), \sum_{i=0}^{1} q'_{\mathrm{f},c}(i) \cdot q'_{\mathrm{f},d}(1-i), \ldots, \sum_{i=0}^{C_u} q'_{\mathrm{f},c}(i) \cdot q'_{\mathrm{f},d}(C_u - i) \right\}. \tag{27}$$

Finally, the computation of, $q'_{\mathrm{f},u,w}$, is based on $q_{\mathrm{f},u,w} = Q^{u,w}_{\mathrm{f},(-1)} * q'_{\mathrm{f},u,w,1}$ and the normalization $q'_{\mathrm{f},u,w}(j) = q_{\mathrm{f},u,w}(j)/G_{\mathrm{f},u,w}$ with $G_{\mathrm{f},u,w} = \sum_{j=0}^{C_u} q_{\mathrm{f},u,w}(j)$.

Step B

In this step, we proceed with the calculation of the aggregated o.d. of all RRHs without taking into consideration the u,w-th one, via:

$$Q_{\mathrm{f},(-(u,w))} = q'_{\mathrm{f},1,1} * \ldots * q'_{\mathrm{f},u,w-1} * q'_{\mathrm{f},u,w+1} * \ldots * q'_{\mathrm{f},U,W_U}. \tag{28}$$

The operation of $q'_{\mathrm{f},v}$ and $q'_{\mathrm{f},w}$ is given by (12), while the normalized values of $Q_{\mathrm{f},(-(u,w))}(j)$, $Q'_{\mathrm{f},(-(u,w))}(j)$, can be determined via $Q'_{\mathrm{f},(-(u,w))}(j) = Q_{\mathrm{f},(-(u,w))}(j)/G_{\mathrm{f},(-(u,w))}$ where $G_{\mathrm{f},(-(u,w))} = \sum_{j=0}^{T} Q_{\mathrm{f},(-(u,w))}(j)$.

Step C

Herein, we calculate $Q'_{\mathrm{f},(-(u,w))} * q'_{\mathrm{f},u,w}$. The latter leads to the un-normalized $Q_{\mathrm{f},u,w}(j)$ which can be normalized via: $G^*_{\mathrm{f},u,w} = \sum_{j=0}^{T} Q_{\mathrm{f},u,w}(j)$:

$$Q'_{\mathrm{f}}(j) = \frac{Q_{\mathrm{f},u,w}(j)}{G^*_{\mathrm{f},u,w}}. \tag{29}$$

To determine the values of $Q'_{\mathrm{f}}(j)$, one may choose any of the u,w RRHs since all of them have the same capacity and o.d.

Based on (29), we can now calculate the TC probabilities due to the CRUs and RRUs unavailability, via: (30) and (31), respectively:

$$B^{\mathrm{TC}}_{\mathrm{c},u,w,s} = \sum_{j=T-b^{\mathrm{c}}_{u,w,s}+1}^{T} Q'_{\mathrm{f}}(j), \tag{30}$$

$$B^{\mathrm{TC}}_{\mathrm{r},u,w,s} = \frac{1}{G^*_{\mathrm{f},u,w}} \sum_{x=C_u-b^{\mathrm{r}}_{u,w,s}+1}^{C_u} q'_{\mathrm{f},u,w}(x) \sum_{y=x}^{T-b^{\mathrm{r}}_{u,w,s}} Q'_{\mathrm{f},(-(u,w))}(T - b^{\mathrm{r}}_{u,w,s} - y). \tag{31}$$

5. Conclusions

Two new multi-rate loss models are proposed in this work, namely the f-MC-SC and the f-MC-MC models, for the analysis of a C-RAN that accommodates different service classes of calls which arrive in the system according to a quasi-random process. The f-MC-SC model describes a C-RAN of a single cluster of RRHs while the f-MC-MC model includes multiple clusters of RRHs (clusters are distinguished via the RRH capacity in radio RUs). We proved that a PFS exists for both models and proposed convolution algorithms for the efficient determination of TC probabilities. The accuracy of these algorithms was verified via simulation. The main conclusions of our work are (a) that the behaviour (in terms of TC probabilities) of the proposed f-MC-SC model cannot be captured by the existing f-SC-SC model and (b) that the total TC probabilities increase as the offered traffic-load increases.

As a future extension of this paper, we intend to study similar C-RAN structures but for bursty traffic and elastic type calls [60–64]. In the case of bursty traffic, a possible idea is to express the notion of burstiness via the compound Poisson process where calls arrive in the RRHs as batches (a batch contains one or more calls of the same service class) while batches follow a Poisson process. Regarding the case of elastic type calls we may consider two different scenarios: (a) a call may have different (elastic) resource requirements during the call set-up phase and use certain (fixed) RUs while in service and (b) a call may have certain (min and max) resource requirements during the call set up phase and use, while in service, RUs that fluctuate between these min and max values. Following these two main extensions, a possible future direction can be the study of more complicated resource sharing policies in C-RAN architectures such as the multiple fractional channel reservation policy and the probabilistic threshold policy which may provide a better handling of congestion probabilities from the network planning point of view [33,65].

An additional aspect that can be included in our models is the notion of quality of experience (QoE). The QoE concept has emerged due to the progress of multimedia services, such as online 4K streaming video and virtual reality, along with diverse capabilities of devices through which such services are used [66]. The NFV may enable network management to be automated and at the same time ensure that the QoE/QoS requirements of the end users are fulfilled [67]. In any case, and to the best of our knowledge, there are no C-RAN teletraffic models that provide congestion probabilities formulas which consider both QoS and QoE requirements.

Author Contributions: Conceptualization, all authors; methodology, all authors; software, I.-A.C. and I.M.; validation, I.-A.C. and I.M.; writing—original draft preparation, all authors; writing—review and editing, all authors. All authors have read and agreed to the published version of the manuscript.

Funding: This research received no external funding.

Conflicts of Interest: The authors declare no conflict of interest.

References

1. Checko, A.; Christiansen, H.L.; Yan, Y.; Scolari, L.; Kardaras, G.; Berger, M.S.; Dittmann, L. Cloud RAN for Mobile Networks—A Technology Overview. *IEEE Commun. Surv. Tutor.* **2015**, *17*, 405–426. [CrossRef]
2. Zhu, M.; Gu, J.; Zeng, X.; Yan, C.; Gu, P. Delay-Aware Energy-Saving Strategies for BBU Pool in C-RAN: Modeling and Optimization. *IEEE Access* **2021**, *9*, 63257–63266. [CrossRef]
3. Alimi, I.; Teixeira, A.; Monteiro, P. Toward an Efficient C-RAN Optical Fronthaul for the Future Networks: A Tutorial on Technologies, Requirements, Challenges, and Solutions. *IEEE Commun. Surv. Tutor.* **2018**, *20*, 708–769. [CrossRef]
4. Aqeeli, E.; Moubayed, A.; Shami, A. Power-Aware Optimized RRH to BBU Allocation in C-RAN. *IEEE Trans. Wirel. Commun.* **2018**, *17*, 1311–1322. [CrossRef]
5. Pliatsios, D.; Sarigiannidis, P.; Goudos, S.; Karagiannidis, G. Realizing 5G vision through Cloud RAN: Technologies, challenges, and trends. *EURASIP J. Wirel. Commun. Netw.* **2018**, *2018*, 136. [CrossRef]
6. Rodoshi, R.T.; Kim, T.; Choi, W. Resource Management in Cloud Radio Access Network: Conventional and New Approaches. *Sensors* **2020**, *20*, 2708. [CrossRef]
7. Mohammedali, N.A.; Kanakis, T.; Agyeman, M.O.; Al-Sherbaz, A. A Survey of Mobility Management as a Service in Real-Time Inter/Intra Slice Control. *IEEE Access* **2021**, *9*, 62533–62552. [CrossRef]
8. Mukhlif, F.; Noordin, K.; Mansoor, A.; Kasirun, Z. Green transmission for C-RAN based on SWIPT in 5G: A review. *Wirel. Netw.* **2019**, *25*, 2621–2649. [CrossRef]
9. Wang, L.; Zhou, S. On the Fronthaul Statistical Multiplexing Gain. *IEEE Commun. Lett.* **2017**, *21*, 1099–1102. [CrossRef]
10. Larsen, L.; Checko, A.; Christiansen, H. A Survey of the Functional Splits Proposed for 5G Mobile Crosshaul Networks. *IEEE Commun. Surv. Tutor.* **2019**, *21*, 146–172. [CrossRef]
11. Ismail, T.; Mahmoud, H.H.M. Optimum Functional Splits for Optimizing Energy Consumption in V-RAN. *IEEE Access* **2020**, *8*, 194333–194341. [CrossRef]
12. Ahmad, I.; Kumar, T.; Liyanage, M.; Okwuibe, J.; Ylianttila, M.; Gurtov, A. Overview of 5G Security Challenges and Solutions. *IEEE Commun. Stand. Mag.* **2018**, *2*, 36–43. [CrossRef]
13. Santoyo-González, A.; Cervelló-Pastor, C. Network-Aware Placement Optimization for Edge Computing Infrastructure Under 5G. *IEEE Access* **2020**, *8*, 56015–56028. [CrossRef]

14. Dai, B.; Yu, W. Energy Efficiency of Downlink Transmission Strategies for Cloud Radio Access Networks. *IEEE J. Sel. Areas Commun.* **2016**, *34*, 1037–1050. [CrossRef]
15. Li, Y.; Jiang, T.; Luo, K.; Mao, S. Green Heterogeneous Cloud Radio Access Networks: Potential Techniques, Performance Trade-offs, and Challenges. *IEEE Commun. Mag.* **2017**, *55*, 33–39. [CrossRef]
16. Tian, B.; Zhang, Q.; Li, Y.; Tornatore, M. Joint Optimization of Survivability and Energy Efficiency in 5G C-RAN With mm-Wave Based RRH. *IEEE Access* **2020**, *8*, 100159–100171. [CrossRef]
17. Masoudi, M.; Lisi, S.S.; Cavdar, C. Cost-Effective Migration Toward Virtualized C-RAN With Scalable Fronthaul Design. *IEEE Syst. J.* **2020**, *14*, 5100–5110. [CrossRef]
18. Ferrus, R.; Sallent, O.; Perez-Romero, J.; Agusti, R. On 5G Radio Access Network Slicing: Radio Interface Protocol Features and Configuration. *IEEE Commun. Mag.* **2018**, *56*, 184–192. [CrossRef]
19. AlQahtani, S.; Alhomiqani, W. A multi-stage analysis of network slicing architecture for 5G mobile networks. *Telecommun. Syst.* **2020**, *73*, 205–221. [CrossRef]
20. Shen, X.; Gao, J.; Wu, W.; Lyu, K.; Li, M.; Zhuang, W.; Li, X.; Rao, J. AI-Assisted Network-Slicing Based Next-Generation Wireless Networks. *IEEE Open J. Veh. Technol.* **2020**, *1*, 45–66. [CrossRef]
21. Liu, J.; Zhou, S.; Gong, J.; Niu, Z.; Xu, S. On the statistical multiplexing gain of virtual base station pools. In Proceedings of the 2014 IEEE Global Communications Conference, Austin, TX, USA, 8–12 December 2014; pp. 2283–2288. [CrossRef]
22. Avramova, A.; Christiansen, H.; Iversen, V. Cell Deployment Optimization for Cloud Radio Access Networks using Teletraffic Theory. In Proceedings of the Fifth International Conference on Advanced Communications and Computation, Brussels, Belgium, 21–26 June 2015; pp. 96–101.
23. Checko, A.; Avramova, A.; Berger, M.; Christiansen, H. Evaluating C-RAN fronthaul functional splits in terms of network level energy and cost savings. *J. Commun. Netw.* **2016**, *18*, 162–172. [CrossRef]
24. Liu, J.; Zhou, S.; Gong, J.; Niu, Z.; Xu, S. Statistical Multiplexing Gain Analysis of Heterogeneous Virtual Base Station Pools in Cloud Radio Access Networks. *IEEE Trans. Wirel. Commun.* **2016**, *15*, 5681–5694. [CrossRef]
25. Chousainov, I.A.; Moscholios, I.; Sarigiannidis, P.; Kaloxylos, A.; Logothetis, M. An analytical framework of a C-RAN supporting random, quasi-random and bursty traffic. *Comput. Netw.* **2020**, *180*, 107410. [CrossRef]
26. Chousainov, I.A.; Moscholios, I.D.; Sarigiannidis, P.G. Congestion Probabilities in a Multi-Cluster C-RAN Servicing a Mixture of Traffic Sources. *Electronics* **2020**, *9*, 2120. [CrossRef]
27. Chousainov, I.A.; Moscholios, I.; Kaloxylos, A.; Logothetis, M. Performance Evaluation of a C-RAN Supporting Quasi-Random Traffic. In Proceedings of the 2019 International Conference on Software, Telecommunications and Computer Networks (SoftCOM), Split, Croatia, 19–21 September 2019; pp. 1–6. [CrossRef]
28. Chousainov, I.A.; Moscholios, I.; Kaloxylos, A.; Logothetis, M. Performance Evaluation in Single or Multi-Cluster C-RAN Supporting Quasi-Random Traffic. *J. Commun. Softw. Syst.* **2020**, *16*, 170–179. [CrossRef]
29. Stasiak, M.; Głąbowski, M.; Wisniewski, A.; Zwierzykowski, P. *Modeling and Dimensioning of Mobile Networks: From GSM to LTE*; John Wiley: Hoboken, NJ, USA, 2011; [CrossRef]
30. Moscholios, I.; Logothetis, M. *Efficient Multirate Teletraffic Loss Models beyond Erlang*; JohnWiley & IEEE Press: Hoboken, NJ, USA, 2019. [CrossRef]
31. Moscholios, I.; Logothetis, M.; Boucouvalas, A. Blocking probabilities of elastic and adaptive calls in the Erlang multirate loss model under the threshold policy. *Telecommun. Syst.* **2016**, *62*, 245–262. [CrossRef]
32. Głąbowski, M.; Kaliszan, A.; Stasiak, M. Modelling overflow systems with distributed secondary resources. *Comput. Netw.* **2016**, *108*, 171–183. [CrossRef]
33. Moscholios, I.; Vassilakis, V.; Logothetis, M.; Boucouvalas, A. State-dependent bandwidth sharing policies for wireless multirate loss networks. *IEEE Trans. Wirel. Commun.* **2017**, *16*, 5481–5497. [CrossRef]
34. Vassilakis, V.; Moscholios, I.; Logothetis, M. Efficient radio resource allocation in SDN/NFV based mobile cellular networks under the complete sharing policy. *IET Netw.* **2018**, *7*, 103–108. [CrossRef]
35. Hanczewski, S.; Stasiak, M.; Weissenberg, J. Queueing model of a multi-service system with elastic and adaptive traffic. *Comput. Netw.* **2018**, *147*, 146–161. [CrossRef]
36. Moscholios, I.; Vassilakis, V.; Sagias, N.; Logothetis, M. On Channel Sharing Policies in LEO Mobile Satellite Systems. *IEEE Trans. Aerosp. Electron. Syst.* **2018**, *54*, 1628–1640. [CrossRef]
37. Panagoulias, P.; Moscholios, I. Congestion probabilities in the X2 link of LTE Networks. *Telecommun. Syst.* **2019**, *17*, 585–599. [CrossRef]
38. Głąbowski, M.; Kaliszan, A.; Stasiak, M. A Palm-Jacobaeus Loss Formula for Multi-Service Systems with Separated Resources. *Appl. Sci.* **2020**, *10*, 4019. [CrossRef]
39. Głąbowski, M.; Sobieraj, M.; Stasiak, M.; Dominik Stasiak, M. Modeling of Clos Switching Structures with Dynamically Variable Number of Active Switches in the Spine Stage. *Electronics* **2020**, *9*, 1073. [CrossRef]
40. Panagoulias, P.; Moscholios, I.; Sarigiannidis, P.; Logothetis, M. Congestion probabilities in OFDM wireless networks with compound Poisson arrivals. *IET Commun.* **2020**, *14*, 674–681. [CrossRef]
41. Głąbowski, M.; Leitgeb, E.; Sobieraj, M.; Stasiak, M. Analytical Modeling of Switching Fabrics of Elastic Optical Networks. *IEEE Access* **2020**, *8*, 193462–193477. [CrossRef]

42. Głąbowski, M.; Kmiecik, D.; Stasiak, M. On Increasing the Accuracy of Modeling Multi-Service Overflow Systems with Erlang-Engset-Pascal Streams. *Electronics* **2021**, *10*, 508. [CrossRef]
43. Yan, F.; Maillé, P.; Lagrange, X. Performance analysis of cellular networks with delay tolerant users. *Telecommun. Syst.* **2021**, *77*, 241–253. [CrossRef]
44. Wang, X.; Gao, L. *When 5G Meets Industry 4.0*; Springer Nature: Singapore, 2020. [CrossRef]
45. Kim, D.; Kim, S. Network slicing as enablers for 5G services: State of the art and challenges for mobile industry. *Telecommun. Syst.* **2019**, *71*, 517–527. [CrossRef]
46. Chousainov, I.A.; Moscholios, I.; Sarigiannidis, P.; Logothetis, M. Multiservice Loss Models for Cloud Radio Access Networks. *IEEE Access* **2021**. [CrossRef]
47. Głąbowski, M.; Kaliszan, A.; Stasiak, M. On the Application of the Asymmetric Convolution Algorithm in Modeling of Full-Availability Group with Bandwidth Reservation. In *International Teletraffic Congress*; Springer: Berlin/Heidelberg, Germany, 2007; Volume 4516, pp. 878–889. [CrossRef]
48. Głąbowski, M.; Kaliszan, A.; Stasiak, M. Convolution Algorithm for State-Passage Probabilities Calculation in Limited-Availability Group. In Proceedings of the Fourth Advanced International Conference on Telecommunications, Athens, Greece, 8–13 June 2008; pp. 215–220. [CrossRef]
49. Huang, Q.; Ko, K.T.; Iversen, V.B. A new convolution algorithm for loss probability analysis in multiservice networks. *Perform. Eval.* **2011**, *68*, 76–87. [CrossRef]
50. Hanczewski, S.; Kaliszan, A.; Stasiak, M. Convolution model of a queueing system with the cFIFO service discipline. *Mob. Inf. Syst.* **2016**, *2016*, 2185714. [CrossRef]
51. Moscholios, I.; Vassilakis, V.; Logothetis, M.; Boucouvalas, A. A Probabilistic Threshold-Based Bandwidth Sharing Policy for Wireless Multirate Loss Networks. *IEEE Wirel. Commun. Lett.* **2016**, *5*, 304–307. [CrossRef]
52. Sagkriotis, S.; Pantelis, S.; Moscholios, I.; Vassilakis, V. Call blocking probabilities in a two-link multirate loss system for Poisson traffic. *IET Netw.* **2018**, *7*, 233–241. [CrossRef]
53. Sopin, E.; Ageev, K.; Markova, E.; Vikhrova, O.; Gaidamaka, Y. Performance Analysis of M2M Traffic in LTE Network Using Queuing Systems with Random Resource Requirements. *Autom. Control. Comput. Sci.* **2018**, *52*, 345–353. [CrossRef]
54. Efrosinin, D.; Stepanova, N. Estimation of the Optimal Threshold Policy in a Queue with Heterogeneous Servers Using a Heuristic Solution and Artificial Neural Networks. *Mathematics* **2021**, *9*, 1267. [CrossRef]
55. Rice, S.; Marjanski, A.; Markowitz, H.; Bailey, S. The SIMSCRIPT III programming language for modular object-oriented simulation. In Proceedings of the Winter Simulation Conference, Orlando, FL, USA, 4 December 2005. [CrossRef]
56. Jain, R. *The Art of Computer Systems Performance Analysis*; John Wiley & Sons: Hoboken, NJ, USA, 1991.
57. Robinson, S. A statistical process control approach to selecting a warm-up period for a discrete-event simulation. *Eur. J. Oper. Res.* **2007**, *176*, 332–346. [CrossRef]
58. Johnson, S.A. A performance analysis of integrated communications systems. *Br. Telecom Technol. J.* **1985**, *3*, 36–45.
59. Moscholios, I.; Vardakas, J.; Logothetis, M.; Boucouvalas, A. New Algorithms for Performance Measures Derivatives in the Erlang Multirate Loss Model including the Bandwidth Reservation Policy. *Mediterr. J. Comput. Netw.* **2011**, *7*, 304–316.
60. Moscholios, I.D.; Logothetis, M.D.; Kokkinakis, G.K. Connection-Dependent Threshold Model: A Generalization of the Erlang Multiple Rate Loss Model. *Perform. Eval.* **2002**, *48*, 177–200. [CrossRef]
61. Moscholios, I.D.; Logothetis, M.D.; Nikolaropoulos, P.I. Engset Multi-Rate State-Dependent Loss Models. *Perform. Eval.* **2005**, *59*, 247–277. [CrossRef]
62. Glabowski, M.; Sobieraj, M.; Stasiak, M. A full-availability group model with multi-service sources and threshold mechanisms. In Proceedings of the 8th International Symposium on Communication Systems, Networks Digital Signal Processing (CSNDSP), Poznan, Poland, 18–20 July 2012; pp. 1–5. [CrossRef]
63. Moscholios, I.; Vardakas, J.; Boucouvalas, A. Congestion Probabilities in a Batched Poisson Multirate Loss Model Supporting Elastic and Adaptive Traffic. *Ann. Telecommun.* **2012**, *68*, 327–344. [CrossRef]
64. Hanczewski, S.; Stasiak, M.; Weissenberg, J. A Model of a System With Stream and Elastic Traffic. *IEEE Access* **2021**, *9*, 7789–7796. [CrossRef]
65. Vazquez-Avila, J.; Cruz-Perez, F.; Ortigoza-Guerrero, L. Performance analysis of fractional guard channel policies in mobile cellular networks. *IEEE Trans. Wirel. Commun.* **2006**, *5*, 301–305. [CrossRef]
66. Bouraqia, K.; Sabir, E.; Sadik, M.; Ladid, L. Quality of Experience for Streaming Services: Measurements, Challenges and Insights. *IEEE Access* **2020**, *8*, 13341–13361. [CrossRef]
67. Barakabitze, A.A.; Barman, N.; Ahmad, A.; Zadtootaghaj, S.; Sun, L.; Martini, M.G.; Atzori, L. QoE Management of Multimedia Streaming Services in Future Networks: A Tutorial and Survey. *IEEE Commun. Surv. Tutor.* **2020**, *22*, 526–565. [CrossRef]